# UWB antipodal Vivaldi antenna for monostatic configuration of through wall imaging applications

SAJJAD AHMED[1,2,3], ARIFFUDDIN JORET[1,3,*], NORSHIDAH KATIRAN[1], ASMARASHID PONNIRAN[1], M. F. L. ABDULLAH[1], ZAHRILADHA ZAKARIA[4], MUHAMMAD SUHAIMI SULONG[5]
[1]*Faculty of Electrical and Electronic Engineering, Universiti Tun Hussein Onn Malaysia (UTHM), Johor, Malaysia*
[2]*Faculty of Science, Quaid-e-Awam University of Engineering, Science and Technology (QUEST) Nawabshah, Pakistan*
[3]*Internet of Things Focus Group, Universiti Tun Hussein Onn Malaysia, (UTHM), Johor, Malaysia*
[4]*Universiti Teknikal Malaysia Melaka, (UTeM), Melaka, Malaysia*
[5]*Faculty of Technical and Vocational Education, Universiti Tun Hussein Onn Malaysia, (UTHM), Johor, Malaysia*

This article presents an ultra-wideband (UWB) corrugated slit antipodal Vivaldi antenna (CS-AVA) for through wall imaging (TWI) applications. The antenna was designed using Rogers RT-Duroid 5880 material with corrugated slits applied on flares of antipodal Vivaldi antenna (AVA) to improve performance. The proposed antenna operated in frequency band (3.1 GHz to 10.6 GHz) and had reflection coefficient of less than -10 dB. A specific stable gain of around 11.7 dB is achieved with good directivity and fine radiation patterns. Using this monostatic UWB antenna design, a TWI simulation-based experiment was carried out. It has been found that the received signal of the UWB-AVA can be used to detect metallic objects through the wall.

(Received August 10, 2022; accepted April 10, 2024)

*Keywords:* Through wall imaging (TWI), Antipodal Vivaldi antenna (AVA), Ultra-wideband (UWB), Antenna received signal

## 1. Introduction

Through wall imaging (TWI) technology has become increasingly demanding in recent years as a result of the increased interest among researchers in discovering what is located behind walls. The TWI approaches are highly desirable for a wide range of applications, including military, police, rescue operations and public safety. For instance, the TWI can be utilized by the police and the military to locate concealed items such as bombs, firearms, and other types of explosive materials [1]. It also makes it possible for rescue teams to identify signs of life at the scene of an earthquake [2], and it can be used in mines in situations where miners are trapped underground [3].

Through wall imaging (TWI) refers to a system that can detect things of interest behind a wall or in a closed environment. The radio frequency (RF) signal is delivered via a transmitted antenna, penetrates the wall, is reflected by the target object, and then again penetrates the wall and is received via a receiving antenna. Signal processing techniques are applied to this reflected signal in order to extract information from behind the barriers. Most of the latest generation TWI systems use UWB technology. UWB technology was chosen due to its high image resolution, good obstacle penetration, high data rates, low power consumption, [4] and higher working bandwidth. This makes the UWB based TWI system a good contender for detecting, locating, and imaging targets behind a wall or in a confined space.

UWB based TWI techniques have numerous applications, including surveillance, defence, public safety, life detection, and medical health monitoring [5-6]. There is great concern regarding the use of UWB-TWI technology to identify hidden or through-wall targets. TWI methods are highly desirable for detecting metal-based explosive objects in congested public places such as airports, hospitals, sports arena parks, and shopping malls for security purposes. Vivaldi antennas are the most popular choice for through-wall detection and imaging, as they meet most of the necessary parameters. The Vivaldi antenna has the following advantages: small size, high gain, higher bandwidth, higher directivity, lower cost, low side lobes, and end-fire radiation [7-8]. Researchers have proposed UWB Vivaldi antennas for TWI applications. Published in [9] is the Vivaldi antenna-based imaging system created for detection of hidden metal objects.

Designing UWB antennas for the TWI technique is an emerging field of study. The UWB antenna works as a sensor element for the TWI system [10-11]. The antenna's performance is crucial to the system as a whole. Dr. Gazit first invented the antenna, which is an antipodal Vivaldi antenna (AVA), in 1988 [12]. In designing this antenna, both Vivaldi flares are antipodal, meaning they are on opposite sides of the substrate. The upper flare, also known as the upper patch, serves as a conductor, while the lower flare, also known as the lower patch, serves as a ground. Corrugated structure with slits is widely used in antipodal Vivaldi antenna to improve performance [13-14]. The corrugation structure used similarly shaped slits with repeating patterns on the outer edge of the flares. The corrugated slits on flares of AVA improve gain, bandwidth and return loss. Furthermore, the corrugation slits work as resistive loading, so the maximum field is directed towards the slit region, which improves the radiation characteristics. In [15], Vivaldi antenna of corrugated

design was proposed for TWI systems for the detection and imaging of metal targets behind a wall.

Another flexible corrugated structure Vivaldi antenna for see-through wall applications was reported in [16]. The presented antenna has achieved a gain of 9.7 dB with a maximum efficiency of 98.08%. In addition to tremendous performance of electromagnet (EM) wave generation, size and cost of this antenna is another factor for the TWI system to be considered by researchers. Zhang et al.; [17] purposed compact size handheld through-wall radar (TWR) system based on a Vivaldi antenna. Another study in [18-19], presented a low cost and compact size UWB Vivaldi antenna for the TWR imaging system. The proposed antenna used corrugation and grating structures that provide better gain, directivity, and impedance matching properties for the TWR applications. Impress to the wideband characteristic of AVA, the antenna with variable corrugated slit length is implemented in [20], to improve gain and bandwidth. Corrugations dimensions are optimized to produce a maximum gain and bandwidth of up to 10.4 dBi and 4.40 GHz respectively. Another corrugated AVA with variable length rectangular slots for imaging applications is presented in [21]. The designed antenna showed that the reflection coefficient parameter ($S_{11}$) is less than -10 dB in the whole selected frequency band. Referring to [22], a broadband AVA based on corrugation structure used, manage to achieve gain and bandwidth of up to 9 dBi and 6.37 GHz respectively. AVA flares can be modified with periodic slits to improve overall performance. In the literature [23], trapezoidal shape and periodic slit edge dielectric directors were integrated into the conventional antipodal Vivaldi antenna (CAVA) to construct the periodic slit edge antipodal Vivaldi antenna (PSEAVA) to boost gain and front to back ratio. Another AVA based on corrugated structure for UWB applications were purposed in [24-25].

Considering the uniqueness characteristics of AVA, this paper presents the novel design of UWB AVA with corrugated slit structure for TWI applications. Following that, a TWI simulation model is designed in CST software to detect a metal object located behind a concrete wall. Finally, the simulated TWI model data which is received signal of the antenna is imported from CST into MATLAB software to create a TWI system image showing the correct position of the object model in the simulation.

## 2. Antenna design and simulation based on TWI model

In this work, Fig. 1(a) represents the geometric design of CS-AVA and Fig. 1(b) shows the slit dimension. The excitation of an antenna is carried out by means of a micro strip line of 50 Ω width of 4.56 mm. The CS-AVA is designed and made of RT/Duroid 5880 material. The substrate specification includes substrate thickness of 1.5 mm, dielectric $\varepsilon_r$ value equal to 2.2 and loss tangent ($\delta$) of 0.004. As shown in [26-27], two elliptic curves of the same size were used to produce AVA, and the feeding line and the radiation flared wings are the two primary components. The outer curvature of an antenna wings has an elliptical structure to promote good broadband results, achieved due to smooth expansion between the feeding line and radiation flared wings. An additional seventeen corrugated slits placed on the edges of the antenna at 45 degree with distance of 0.80 mm apart from each corrugated slit. The length of the corrugated slit is 2.75 mm and the width is 1mm.

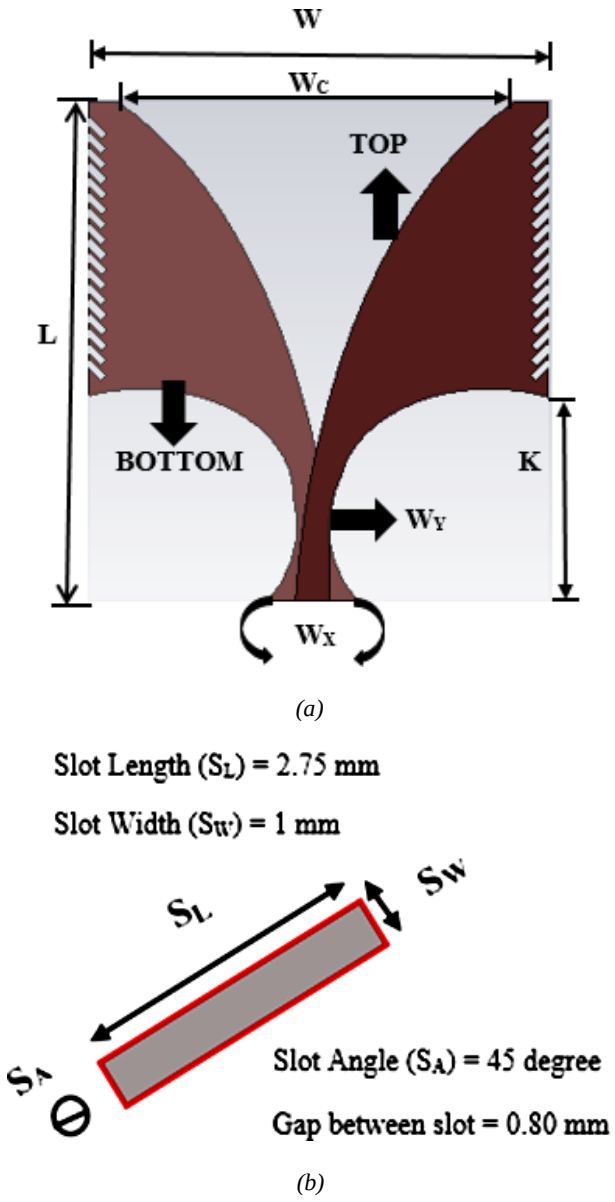


*Fig. 1. CS-AVA design (a) Geometrical design (b) Slit dimension (color online)*

Table 1 shows the optimized dimensions of the design parameters of the CS-AVA antenna that has been carried out in this work. The upper frequency limit of the Vivaldi antenna should theoretically be infinite, whereas the lower frequency limit is determined by the antenna width and the value of the effective dielectric constant ($\varepsilon_{eff}$) as represented by equations (1) and (2) [26].

$$fmin = \frac{c}{2W\sqrt{\varepsilon_{eff}}} \quad (1)$$

$$z_o = \frac{60}{\sqrt{\varepsilon_{eff}}} ln\left(\frac{8h}{w} + \frac{w}{4h}\right) for\left(\frac{w}{h}\right) < 1 \quad (2)$$

$$z_o = \frac{60}{\sqrt{\varepsilon_{eff}}} ln\left(\frac{8h}{w} + \frac{w}{4h}\right) for\left(\frac{w}{h}\right) < 1 \quad (3)$$

$$z_o = \frac{120\pi}{\sqrt{\varepsilon_{eff}}\left[\frac{w}{h} + 1.393 + \frac{2}{3} ln\left(\frac{w}{h} + 1.444\right)\right]} \quad for\left(\frac{w}{h}\right) \geq 1 \quad (4)$$

*Table 1. Dimensions of CS-AVA*

| Dimensions | Value |
|---|---|
| W | 60.75 mm |
| L | 66 mm |
| K | 14 mm |
| $W_C$ | 54.75 mm |
| $W_X$ | 11.75 mm |
| $W_Y$ | 4.56 mm |

The simulation model of the TWI system has been established to observe the detection capability of the CS-AVA as shown in Fig. 2 using CST software. Based on this figure, the EM wave is assumed to be transmitted from the proposed antenna of the monostatic TWI system configuration which penetrates through the concrete wall, hits the target and is reflected back to the same antenna as received signal. In this simulation model configuration, the antenna was moved horizontally in different positions to establish the distance between the antenna and the wall, which was then set at 15 cm. In making the simulation technique of the TWI system reliable, the metallic object is also moved horizontally in different positions to set the distance between it and the wall model, which was also set at 15 cm. In this simulation model, the concrete wall thickness was designed as 10 cm, while its height was set as 14 cm. After successfully determine the best position of the antenna and object, the antenna is then moved vertically in multiple positions to perform a wall scanning procedure to detect the metal object in the CST software simulation model.

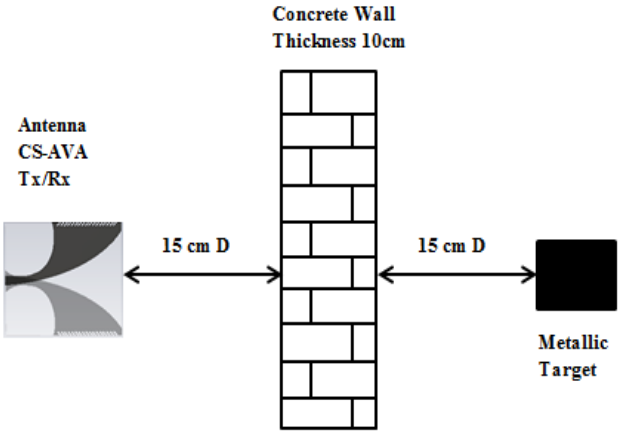


*Fig. 2. Simulation based TWI system by using monostatic Antipodal Vivaldi antenna*

## 3. Results and analysis

In this section, the TWI model and the results of the proposed antenna are analyzed. Fig. 3(a) and 3(b) shows the 3D far-field radiation pattern of the designed CS-AVA at 6.75 GHz and 10 GHz respectively. As can be seen in mentioned figures, the CS-AVA has achieved good gain and directivity values in the UWB frequency range. Exploring the directivity values of the CS-AVA in 2D using polar plot as shown in Fig. 4(a) and 4(b), the proposed antenna can be seen clearly has achieved good directivity values, side lobe levels and angular width. Table 2 shows the detail performance on the designed CS-AVA of this work which includes gain, side lobe level and directivity over selected frequency range. Here, as can be observed that the maximum of gain produced by the CS-AVA is about 11 dB at 10 GHz. The low frequency seems to produce lower value of gain and directivity than the higher. The minimum side lobe level can be achieved at 6 GHz at -11.7 dB.

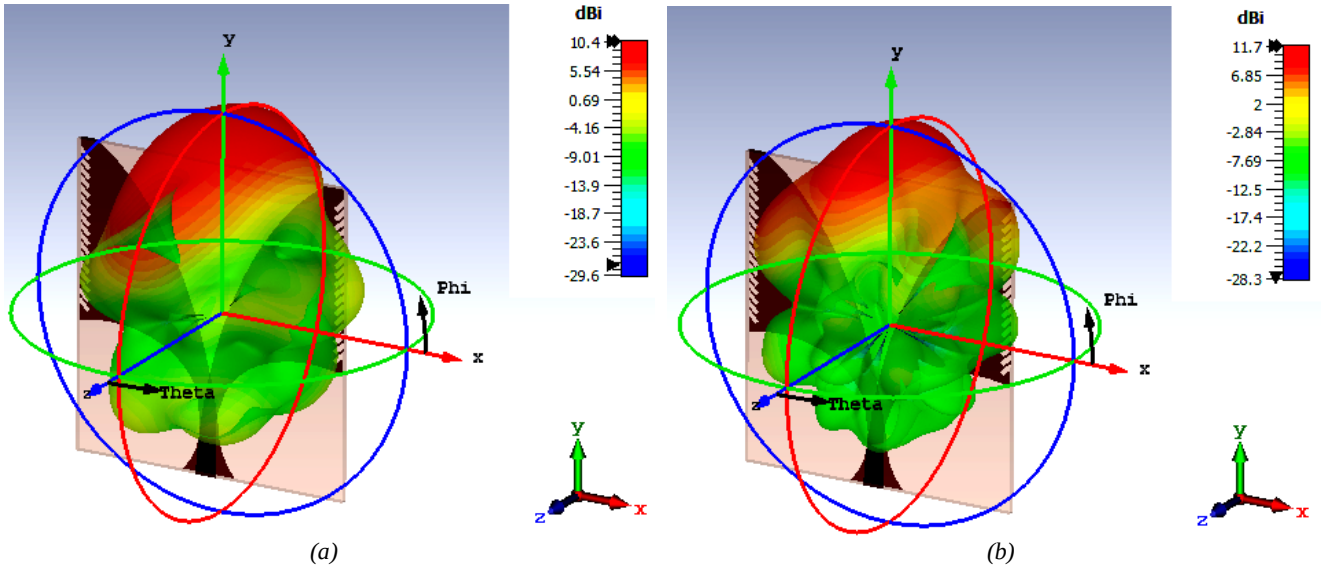


*(a)* *(b)*

*Fig. 3. Far field radiation pattern (a) 6.75 GHz (b) 10 GHz (color online)*

*Table 2. Gain, Directivity and Side lobe levels (SLL) of CS-AVA*

| Frequency | CS-AVA | | |
|---|---|---|---|
| | Gain (dB) | SLL (dBi) | Directivity (dB) |
| 4 GHz | 6.52 | -12.4 | 6.49 |
| 6 GHz | 9.18 | -11.7 | 9.19 |
| 8 GHz | 10.3 | -14.3 | 10.36 |
| 9 GHz | 10.7 | -12.0 | 10.67 |
| 10 GHz | 11.7 | -14.7 | 11.65 |

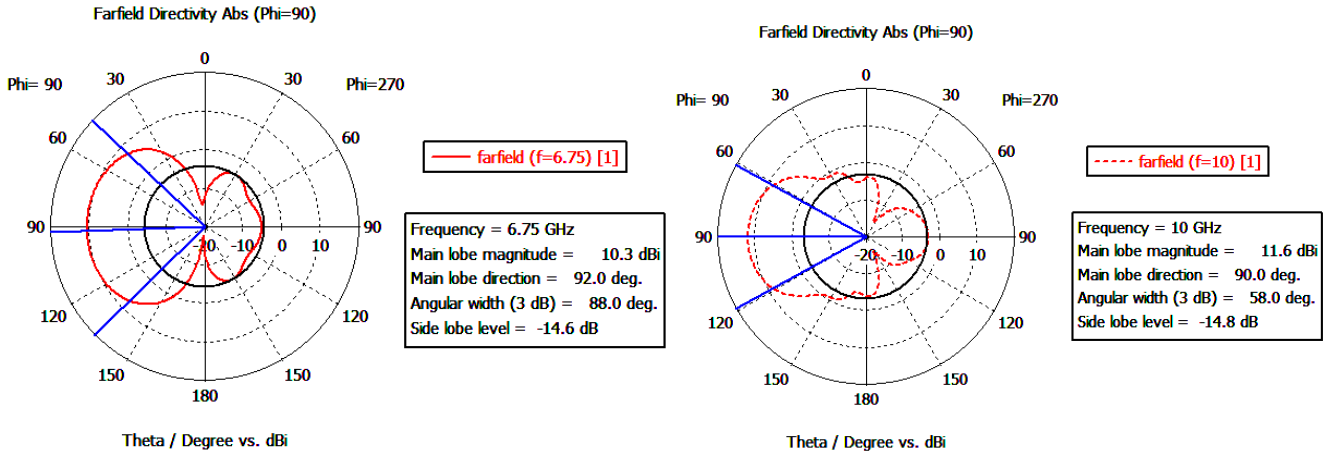


*(a)* *(b)*

*Fig. 4. Polar radiation pattern (a) 6.75 GHz (b) 10 GHz (color online)*

In antenna design technique, $S_{11}$ which is known as reflection parameter of the antenna has been deeply and widely studied by researchers in order to determine the capability of the antenna in transmitting EM wave efficiently. In order to simplify the technique, researchers design a simulation model of the desired antenna using specific antenna design software which implemented various mathematical technique including Finite Different Time Domain (FDTD) and Finite Element (FE). As this work is based on CST software, the mathematical model of the simulation design is based on Finite Integration Technique (FIT). Moreover, as the FIT technique is originally from FDTD technique, it implements time domain calculation which involve time signal. Therefore, the used of antenna received signal depicted from the simulation results beside the $S_{11}$ is equivalent based on

transformation technique of Fast Fourier Transform (FFT). Due to this information, the simulation models designed in this work has focused on the $S_{11}$ and antenna received signal results produced by the CST software. The use of $S_{11}$ in this work is to determine the capability of the designed antenna in producing efficient EM wave, while the use of the antenna received signal is to observe the signal power of the EM wave received by the antenna. S-parameter results of the simulation model of antenna, antenna with wall and antenna with wall and target is shown in Fig. 5, covering the entire UWB band. The $S_{11}$ values produced by the antenna designed along the wall and the target in the UWB band can be considered as able to occupy the selected frequency range with magnitude value below than -6 dB, it consisting of 4 resonance frequency band below -20 dB which are at about 3.2 GHz to 3.7 GHz, 5.7 GHz to 6.1 GHz, 7.7 GHz to 8.6 GHz and 10 GHz to 10.5 GHz. The $S_{11}$ calculation seem to be affected by the wall and target object which produce a shifted value on magnitude of the resonant spectrum with unstable pattern.

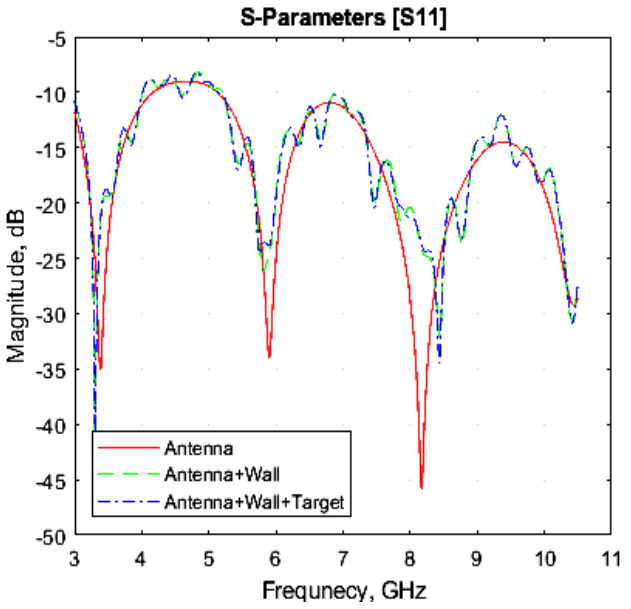


*Fig. 5. Reflection-coefficient ($S_{11}$) of antenna with wall and target*

An electronic system needs a sensor where in TWI system an antenna is used as the sensor to generate and measure the strength of EM wave. Referring to the CST software, the calculated antenna received signal and S-parameters are based on EM wave propagation which is by simulation generated through selected port in the software. The two calculations value can be used to represent the performance of the design antenna in producing and sensing the EM wave. However, as S-parameters represent antenna's characteristic response, the use of the antenna received signal can simplify the EM wave signal calculation. In response to this simplification, Fig. 6 illustrates the transmitted and received signal calculated by the CS-AVA and TWI system model designed in this work. In Fig. 6(a), the peak at 0.5 ns represents the signal transmitted by the antenna, while in Fig. 6(b) the peaks at 0.7 ns and 1.2 ns belong to the antenna received signal. On the other hand, in Fig. 6(c) the amplitude at 2.1 ns and 3.6 ns are the amplitude of the reflections produced by the front and the back of the wall respectively. Meanwhile, in Fig. 6(d) the amplitude at 4.5 ns can be considered as a reflection of the EM wave belongs to the metal object.

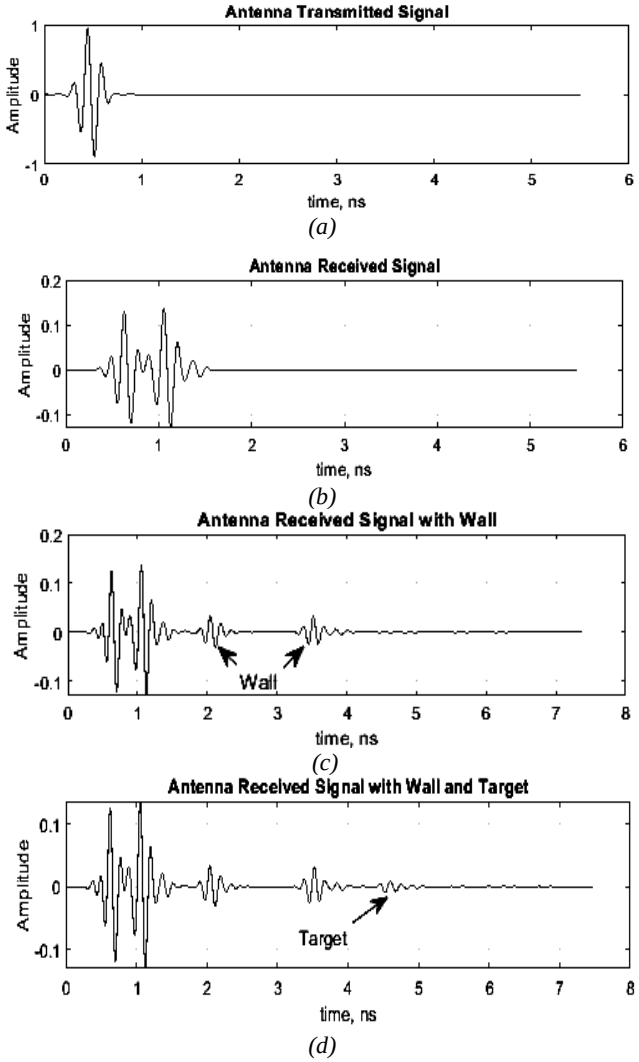


*Fig. 6. Antenna signal transition of TWI experiment (a) Antenna transmitted signal (b) Antenna received signal (c) Antenna received signal with wall (d) Antenna received signal with wall and target*

The capability in detecting hidden object using TWI system can be referred to 2D TWI image produced by the system. In this study, the antenna received signals is transferred from CST software to MATLAB to produce the image. The simulation results comprising the calculation of the received signal of the TWI system antenna in various simulations of the TWI system model with reference to the position of the antenna in the simulation at various points at the level of the wall model, have been arranged in rows to create the TWI 2D system image. Based on the constructed 2D TWI system image, it was observed that the interruption of the signals indicates the existence of the

target through the wall, as shown in Fig. 7(a). Further analyzing the 2D image of the simulation, the antenna received signals was processed using envelope detector signal processing technique known as Asynchronous Full Wave (AFW) [28]. As applying the signal processing technique to the calculated antenna received signals, the target object can be seen clearly as shown in Fig. 7(b) and 7(c).

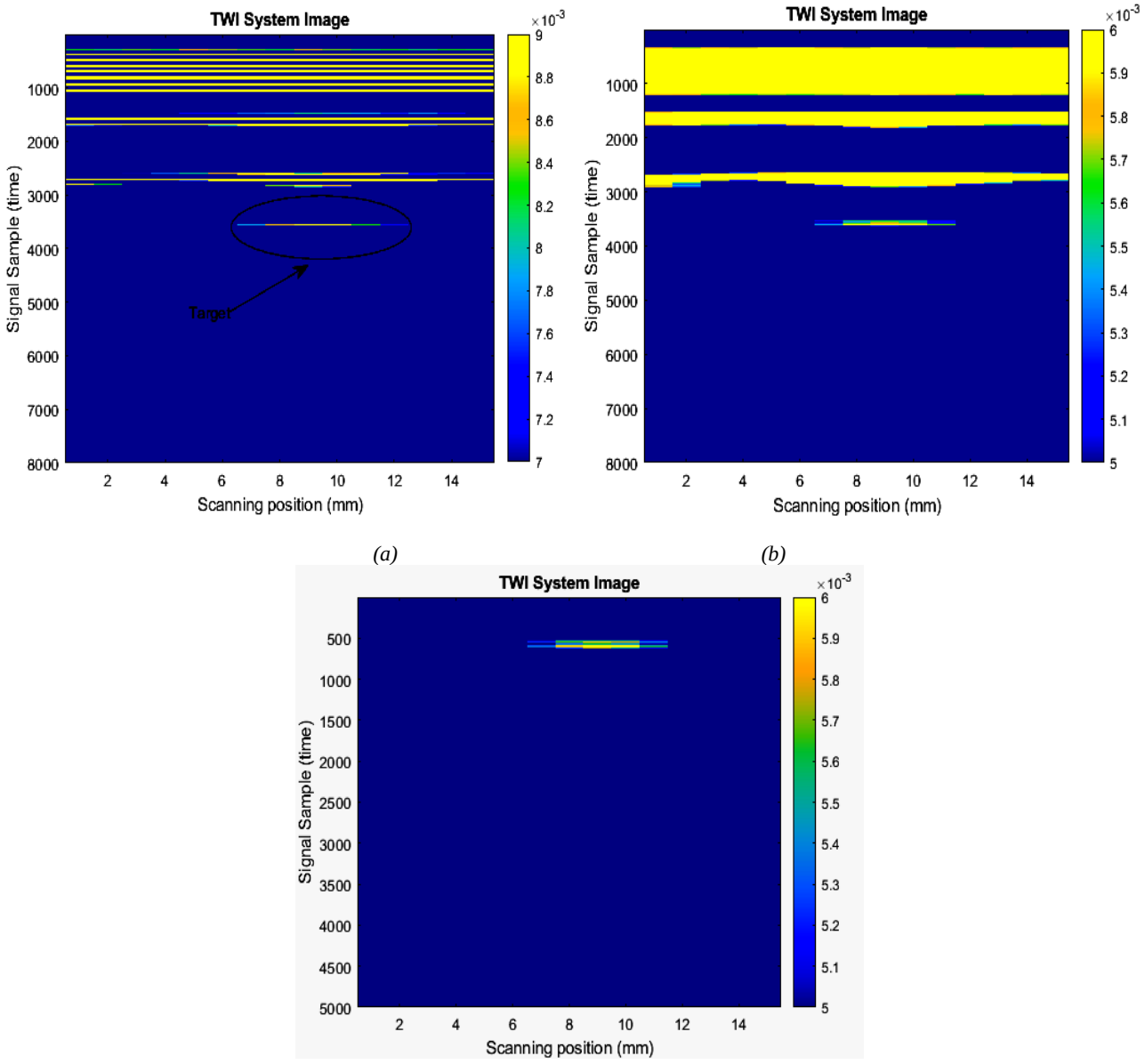


*(a)* *(b)*

*(c)*

*Fig. 7. TWI 2D system image (a) 2D target image (b) 2D target image with envelope detection technique (c) Only target image with envelope detection technique (color online)*

## 4. Conclusion

In this work, a UWB corrugated slit antipodal Vivaldi antenna (CS-AVA) design for through wall imaging (TWI) applications has been presented. This antenna has been simulated in frequency range (3.1 GHz - 10.6 GHz) suitable for through wall scanning and imaging purposes. The addition of corrugated slits in the proposed design has significantly improved the antenna's performance in generating and detecting EM wave. Since then, a simulation-based TWI system has been developed to detect metallic object by using the CS-AVA in monostatic configuration. By using antenna received signal calculated in the simulation, 2D image of the TWI system showing exact position of metal object behind concrete wall is formed. A clear 2D image of the TWI system has been produced as the use of signal processing technique on the received signal, known as Asynchronous Full Wave (AFW) envelope detector. Therefore, it can be concluded that the CS-AVA is a promising candidate for through wall

imaging (TWI) applications and can be explored for other types of TWI system configuration, such as Bistatic and Array.

**Acknowledgements**

This research was supported by the Ministry of Higher Education (MOHE) through Fundamental Research Grant Scheme (FRGS) (FRGS/1/2021/ICT09/UTHM/02/1) and UniversitiTun Hussein Onn Malaysia (UTHM) through Postgraduate Research Assistant Grant (GPPS) (vot H567).

## References

[1] H. Xu, B. Wang, J. Zhang, L. Li, Y. Li, Y. Wang, A. Wang, Sens. Imaging **18**, 6 (2017).
[2] K. Mu, T. H. Laun, L. Zhu, L. X. Cai, L. Gao, IEEE Access **8**, 82951 (2020).
[3] P. K. M. Nkwari, S. Sinha, H. C. Ferreira, IETE Technical Review, **2017**, sept. (2017).
[4] K. J. Babu, R. W. Aldhaheri, L. S. Sai, B. R. Perli, S. R. Pasumarthi, B. K. Kumar, V. N. K. R. Devana, J. Optoelectron. Adv. M. **24**(7-8), 355 (2022).
[5] A. Fedeli, M. Pastorino, C. Ponti, A. Randazzo, G. Schettini, Sensors **20**, 2865 (2020).
[6] M. T. Islam, M. Z. Mahmud, M. T. Islam, S. Kibria, M. Samsuzzaman, Scientific reports **9**, 15491 (2019).
[7] A. Bhattacharjee, A. Bhawal, A. Karmakar, A. Saha, D. Bhattacharya, Int. J. Microw. Wirel. Technol., **2020**, (2020).
[8] M. Elhefnawy, F. Podd, International Journal of Electrical and Computer Engineering Systems **13**, (1) (2022).
[9] Z. Akhter, B. N. Abhijith, M. J. Akhtar, J. Electromagn. Waves Appl. **30**(9), 1183 (2016).
[10] A. T. Mobashsher, K. S. Bialkowski, A. M. Abbosh, S. Crozier, PLOS One, **11**(4), (2016).
[11] M. Z. Mahmud, M. T. Islam, N. Misran, A. F. Almutairi, M. Cho, Sensors **18**, 2951 (2018).
[12] E. Gazit, IEEE Proceedings H (Microwaves, Optics and Antennas) **135**, 89 (1988).
[13] M. Moosazadeh, S. Kharkovsky, J. T. Case B. Samali, IET Microwaves, Antennas and Propagation **11**(6), 796 (2017).
[14] C. F. Liang, C. H. Cheng, IEEE MTT-S Int. Wirel. Symp. (IWS) 2021, May 2021.
[15] B. Kumar, K. A. Vardhan, P. Sharma, 11th Int. Conf. on Industr. and Info. Systems (ICIIS) 704, 2016.
[16] P. Nijhawan, A. Kumar, Y. Dwivedi, 3rd International Conference on Microwave and Photonics (ICMAP 2018), 3, 2018.
[17] J. Zhang, H. Lan, M. Li, Y. Yang, IEEE Sens. J. **20**(8), 4420 (2020).
[18] A. Kuriakose, T. A. George, S. Anand, International Symposium on Antennas and Propagation (APSYM), 58, 2020.
[19] R. R. Menon, S. Najeeb, S. N. Prabhu, T. A. George, A. Kuriakose, Int. Conf. on Communication and Electronics Systems (ICCES), 1096, 2019.
[20] M. Abbak, M. N. Akinci, M. Çayören, I. Akduman, IEEE Trans. Antennas Propag. **65**(6) 3302 (2017).
[21] A. Balaji, J. Karthi, V. Chinnammal, C. Malarvizhi, S. Vanaja, IOP Conf. Ser. Mater. Sci. Eng. **1055**, 012100 (2021).
[22] M. S. Talukder, Md. Samsuzzaman, L. C. Paul, M. A. Masud, R. Azim, M. Moniruzzaman, 24th Int. Conf. Comput. Inf. Technol., (ICCIT) 18, 2021.
[23] M. Moosazadeh, S. Kharkovsky, IEEE Antennas and Wireless Propagation Letters **15**, 552 (2015).
[24] G. K. Pandey, M. K. Meshram, Int. J. RF Microw. Comput. Eng. **25**(7) 610 (2015).
[25] O. Manoochehri, F. Farzami, A. Darvazehban, A. Shamim, H. Bagei, URSI Natl. Radio Sci. Meet. Usn. NRSM 2019.
[26] H. C. Ba, H. Shirai, C. D. Ngoc, IEEE Fifth International Conference on Communications and Electronics (ICCE), Vietnam, 2014.
[27] A. K. Reddy, S.Natarajamani, S. K. Behera, International Conference on Computing, Electronics and Electrical Technologies (ICCEET) 2012.
[28] C. K. N. A. H. C. K. Melor, A. Joret, A. Ponniran, M. S. Sulong, R. Omar, M. Razali, Springer Nature, Lect. Notes Electr. Eng. **666**, 659 (2021).

*Corresponding author: ariff@uthm.edu.my